Understanding the Kinetic and Thermodynamic Origins of Xylene Separation in UiO-66(Zr) via Molecular Simulation

Matthew J. Lennox[†] *and Tina Düren**[§]

† School of Chemistry, University of Nottingham, Nottingham, UK, NG7 2RD

§ Department of Chemical Engineering, University of Bath, Bath, UK, BA2 7AY

ABSTRACT

Xylene isomers are precursors in many important chemical processes, yet their separation via crystallization or distillation is energy intensive. Adsorption presents an attractive, lower-energy alternative and the discovery of adsorbents which outperform the current state-of-the-art zeolitic materials represents one of the key challenges in materials design, with metal-organic frameworks receiving particular attention. One of the most well-studied systems in this context is UiO-66(Zr), which selectively adsorbs *ortho*-xylene over the other C8 alkylaromatics. The mechanism behind this separation has remained unclear, however. In this work, we employ a wide range of computational techniques to explore both the equilibrium and dynamic behavior of the xylene isomers in UiO-66(Zr). In addition to correctly predicting the experimentally-observed *ortho*-selectivity, we demonstrate that the equilibrium selectivity is based upon the complete encapsulation of *ortho*-xylene within the pores of the framework. Furthermore the flexible nature

of the adsorbent is crucial in facilitating xylene diffusion and our simulations reveal for the first time significant differences between the intracrystalline diffusion mechanisms of the three isomers resulting in a kinetic contribution to the selectivity. Consequently it is important to include both equilibrium and kinetic effects when screening MOFs for xylene separations.

INTRODUCTION

In a recent Nature contribution[1], the separation of benzene derivatives and especially xylene isomers was highlighted as one of seven separation processes "to change the world". Xylenes (*para*-, *ortho*- and *meta*-xylene) are di-methyl-substituted aromatic compounds and are necessary precursors in a wide range of chemical processes. Of the isomers, para-xylene (pX) is the most important and used, for example, in the production of polymers such as PET and polyester. The efficient separation of mixtures of xylene isomers into their individual components and the recovery of para-xylene is therefore of great industrial relevance[2]. The majority of pX is produced through adsorption-based separation processes typically using a simulated moving bed (SMB) and a pX-selective, ion-exchanged MFI or FAU zeolite as the adsorbent[2-3]. The efficiency of an SMB for xylene separation depends strongly upon the selectivity and capacity of the adsorbent – the development of more highly pX-selective materials would result in smaller SMB units and lower eluent consumption. Alternatively, a highly *ortho*-selective material in which pX is the least preferred isomer would not only allow the recovery of pX in the raffinate, but also the challenging downstream *ortho*-/*meta*-xylene separation to be avoided[4]. Recently, several metal-organic framework (MOF) structures have been identified which exhibit a strong adsorptive preference for either *ortho*-xylene (oX)[5-9] or pX[10-11], providing potential alternatives to existing zeolitic adsorbents.

Since its discovery in 2008, the zirconium-based MOF UiO-66(Zr)[12] has been the subject of a great deal of interest in the scientific community. Comprised of zirconium oxide clusters connected by benzene dicarboxylate (BDC) linkers, the framework demonstrates excellent chemical, hydrothermal and mechanical stability[12-13], making it an attractive proposition for many industrial applications, including xylene separations[4, 6].

The pore network of UiO-66(Zr) is constructed from larger, octahedral cavities connected by smaller tetrahedral pores (Figure 1). In order to diffuse through the framework, a molecule must pass from one type of pore to the other via a small window of roughly 4 – 5 Å in diameter.

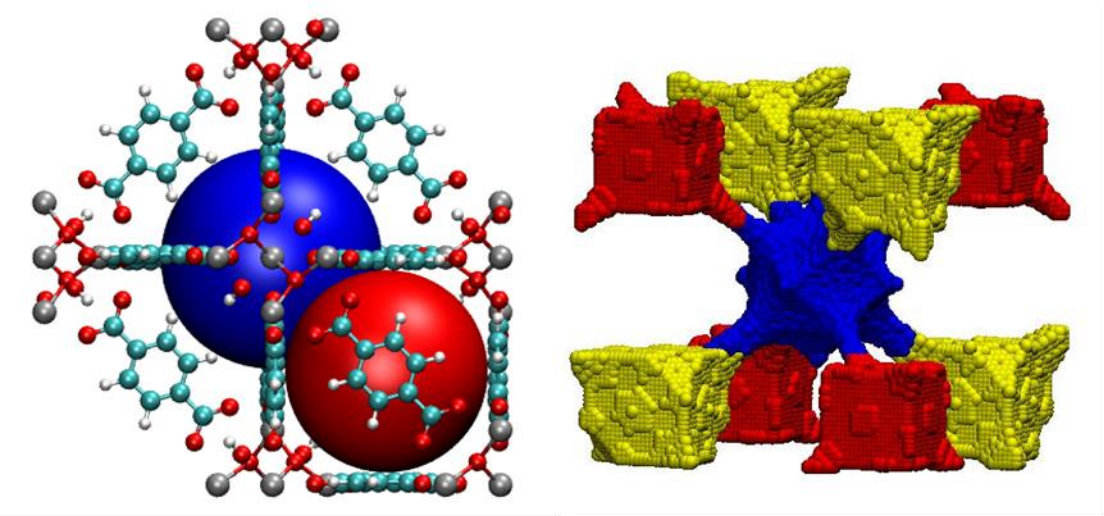

Figure 1 - Pore structure of UiO-66(Zr). The dehydroxylated form of the MOF (left) contains octahedral cavities (blue) surrounded by uniformly sized tetrahedral pores (red). In addition to the central octahedral cavity (blue), hydroxylated UiO-66(Zr) contains two distinct tetrahedral pores (red and yellow in the image on the right). Color scheme: C – cyan; H – white; O – red; Zr – grey.

As-synthesized UiO-66 is fully hydroxylated, with each metal cluster containing four hydroxyl groups alongside eight-coordinated zirconium atoms [$Zr_6O_4(OH)_4$]. Two of these hydroxyl groups along with the remaining two hydrogen atoms can be driven off under heating above 523 K,

producing a de-hydroxylated structure wherein each cluster contains only oxygen and seven-coordinated zirconium atoms $[Zr_6O_6]$[12]. In the case of the hydroxylated UiO-66(Zr), the presence of μ-OH groups results in two distinct types of tetrahedral cavity. The hydroxyl groups are located in the slightly larger of the two tetrahedral cavities (~7.0 Å in diameter). The slightly smaller tetrahedral pores (~6.5 Å in diameter) are devoid of hydroxyl groups. The loss of these μ-OH groups under heating means that only one type of tetrahedral pore (~6.6 Å in diameter) is present in the de-hydroxylated MOF. The window diameter (~4-5 Å) is the same in both forms of UiO-66.

In classical MOF terminology, UiO-66(Zr) is described as being a rigid structure. Even at elevated temperature (up to 648 K), the X-ray diffraction (XRD) data reveals no significant structural flexibility or breathing effects[13]. Although the MOF does not exhibit any large breathing or swelling effects, such as those for example observed in the MIL-53[14] or MIL-88[15] systems, the structure is not static. In UiO-66(Zr) and its functionalised analogues, the primary mode of structural movement is via the rotation or 'flipping' of the BDC linker around its long axis[16-17]. While this linker rotation has little impact on the overall pore size or topology, it has been shown to impact considerably on the diffusion of light gases via modulation of the window size[18].

UiO-66 has been shown experimentally to be selective towards oX[4, 6, 19], exhibiting so-called 'inverse shape selectivity', where - in contrast to more conventionally shape selective MOFs such as MIL-125(Ti) - oX is favoured over the slimmer pX. In the initial adsorption breakthrough studies of Barcia *et al*[6] and Moreira *et al*[4], this preference was attributed to the close match between the diameters of the pores within the MOF and the kinetic diameter of oX, a concept previously described in the separation of linear and branched alkanes in the zeolites SAPO-5[20] and MCM-22[21]. The least rotationally constrained isomer will experience the lowest loss of entropy upon

adsorption, resulting in an overall lower Gibbs free energy of adsorption for species with similar adsorption enthalpies. In the UiO-66(Zr) – xylene system, this effect is expected to manifest itself in an entropic preference for the more compact *ortho*- isomer. This entropic driving force has also been held responsible for the experimentally observed preference of UiO-66(Zr) for branched over linear C_6 isomers[6, 22-23]. More recently, Chang and Yan[19] and Duerinck *et al*[23] have demonstrated experimentally an additional enthalpic preference for *ortho*-xylene, reporting an increased heat of adsorption for oX when compared to mX and pX of 7.5-13.1 kJ/mol, which was suggested to be a result of either favorable interactions between the aromatic rings of oX and the BDC linkers (π-π stacking) or enhanced electrostatic interactions between oX and the μ-OH groups of the MOF.

While the preliminary computational work of Granato *et al*[24] correctly predicted the ortho-selective nature of the MOF and provided reasonable qualitative agreement for measured quantities such as maximum capacity and adsorption enthalpy, the adsorption mechanism and origin of the *ortho*-preference remains unclear. This work, therefore, addresses the fundamental aspects of xylene adsorption and diffusion in UiO-66(Zr) using a range of computational tools and sets out to identify the structural, thermodynamic and kinetic factors which drive the experimentally observed *ortho*-selectivity.

SIMULATION DETAILS

Both the hydroxylated and de-hydroxylated forms of UiO-66(Zr) were considered in this work. The geometry optimized structures of Yang et al, which have been shown to successfully reproduce light gas adsorption isotherms[18, 25], were used. Lennard-Jones parameters for the framework atoms were taken from the DREIDING force field[26] except in the case of zirconium, which is not included in the DREIDING force field and whose parameters were taken from the UFF[27]. Partial charges for the MOFs were calculated following the methods of Yang an co-

workers[28]. Xylene isomers were treated as rigid molecules with all atoms defined explicitly with the exception of methyl groups, which were treated as single spheres. The Lennard-Jones parameters and partial charges were taken from the OPLS force field[29], which has been shown to capture the behavior of xylenes in UiO-66(Zr) well[24].

The adsorption of xylene isomers in UiO-66(Zr) was simulated at 300 K via grand canonical Monte Carlo (GCMC) simulations implemented in the MuSiC software [30]. Xylene molecules were subject to energy-biased insertion and deletion, translation and rotation moves. In the case of mixture simulations, identity swap moves were also included. Single component adsorption isotherms were allowed at least 8 x 10^6 equilibrium steps, followed by 12 x 10^6 production steps for each pressure point, carefully ensuring that equilibrium was reached before starting the sampling process. Mixture simulations were allowed at least 100 x 10^6 steps to come to equilibrium, followed by a further 150 x 10^6 production steps.

The average interaction energy of the different xylene isomers with the framework in each of the pore types in UiO-66(Zr) was studied through Monte Carlo simulations in the NVT ensemble. Simulations were carried with a total of at least 108 xylene molecules (corresponding to one molecule per cavity of interest) and consisted of at least 8 x 10^6 equilibrium steps, followed by 12 x 10^6 production steps. In these simulations, xylene molecules were subjected to random rotation and displacement moves. The starting positions of the xylene molecules were restricted and any displacement which resulted in the center of mass of the molecule entering a neighboring pore was rejected so as only one pore type was explored in each run. The MOF structures were considered to be rigid and atoms were kept fixed at their optimized crystallographic positions in all NVT and μVT Monte Carlo simulations.

The diffusion of xylene isomers in de-hydroxylated UiO-66(Zr) was studied through molecular dynamics (MD) simulations using the DL_Poly Classic package[31]. Initial simulations were carried out with the framework held rigid and the atoms kept fixed in their optimized crystallographic positions for xylene loadings of 3, 6, 9 and 12 molecules/unit cell (uc). In order to assess the impact of framework flexibility on diffusion, further simulations for a xylene loading of 3 molecules/uc were carried out in which the movement of MOF atoms was described using the force field of Yang and co-workers, which has been shown to replicate well the unit cell parameters and equilibrium bond lengths and angles of UiO-66[18, 25]. Both sets of simulations were carried out in the NVT ensemble using a time step of 1 fs. The simulations were allowed at least 0.1 ns to equilibrate before a production run of 10 ns. In the rigid MOF, simulations were carried out at both 300 K and 500 K, while in the flexible MOF, simulations were undertaken at 300 K and at temperatures ranging from 500 – 900 K. In both cases, the Berendsen thermostat was used to control the temperature. The starting positions of the xylene molecules were taken from fully equilibrated GCMC simulations at the appropriate loading.

RESULTS AND DISCUSSION

In line with published experimental data[4, 6], GCMC simulations of binary xylene mixtures show that both de-hydroxylated and hydroxylated forms of UiO-66(Zr) are strongly oX-selective, particularly at low partial pressures (Table 1). While the behaviour of oX-mX mixtures was found to be largely unaffected by the hydroxylation state of the framework, a marked difference in behaviours for mixtures containing pX was observed. Selectivities in pX-containing mixtures exhibited a shift towards pX in the hydroxylated MOF: the hydroxylated MOF was much less selective towards oX for oX-pX mixtures and while the de-hydroxylated MOF was unable to

differentiate between pX and mX (i.e. the selectivity is around 1), the hydroxylated MOF was slightly pX-selective in pX-mX mixture simulations.

Table 1 – Simulated selectivity towards species *a* from equimolar binary mixture *a-b* at 1 Pa and 2 kPa in the hydroxylated and de-hydroxylated forms of UiO-66(Zr).

UiO-66(Zr)	oX-mX		oX-pX		pX-mX	
	1 Pa	2 kPa	1 Pa	2 kPa	1 Pa	2 kPa
Hydroxylated	10.4 ± 0.1	7.1 ± 0.1	9.4 ± 0.1	2.3 ± 0.1	1.6 ± 0.2	3.1 ± 0.1
De-hydroxylated	10.1 ± 0.1	6.4 ± 0.1	12.8 ± 0.1	7.0 ± 0.1	1.1 ± 0.2	1.2 ± 0.3

Examination of the simulated single-component isotherms (Figure 2) reveals that the uptake of pX in the hydroxylated MOF is considerably higher than the other two isomers. This is a result of the larger tetrahedral cavity (which is only present in the hydroxylated form of the MOF) being able to accommodate two pX molecules in GCMC simulations, compared to only a single oX or mX molecule (see Figure S2). While the formation of a pX dimer is geometrically possible in this cavity, it is extremely unlikely that it is accessible in reality, where diffusional limitations will prevent a second pX molecule from entering the cavity should the cavity already be occupied. Given that there is no experimental evidence to indicate an enhanced uptake of pX compared to the other two isomers, this phenomenon is likely to be an artefact introduced by the GCMC simulation technique. (Note that while our simulations mimic pure component vapor phase adsorption or liquid phase adsorption from a non-adsorbing solvent, the available experimental data is either competitive xylene adsorption at elevated temperature[6] or pseudo-single component from a co-adsorbing solvent[4] and a direct comparison is therefore not possible). While dimer formation of only one of the isomers would lead to an enhanced selectivity and may be a suitable

search criteria for adsorbents with improved performance for xylene separations, further analysis in this work will focus on the de-hydroxylated MOF, where the pX dimer is not observed in simulation and the simulation results are free from this un-physical skew towards pX.

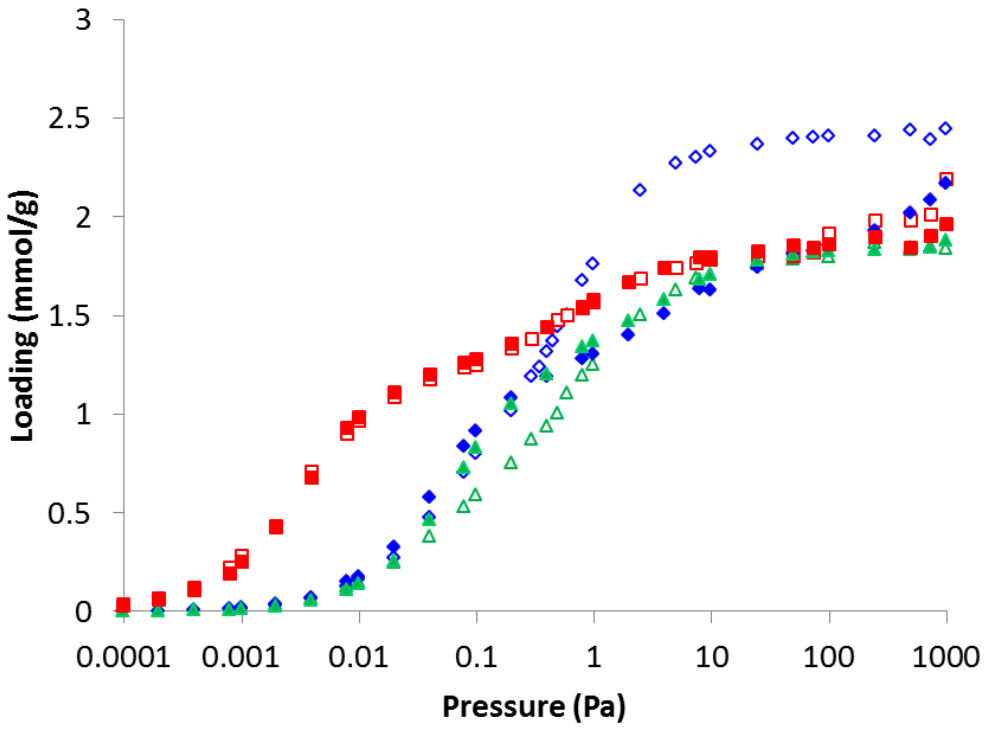

Figure 2 - Simulated single-component isotherms of pX (blue), mX (green) and oX (red) in de-hydroxylated UiO-66(Zr) at 300 K (solid symbols) and in hydroxylated UiO-66(Zr) (empty symbols).

Commensurate with the high oX-selectivity observed in binary GCMC simulations, the low pressure uptake of oX in single-component isotherms is considerably enhanced compared to the other two isomers, which is in qualitative agreement with the experimental work of Moreira *et al* [4]. The isotherms of pX and mX in de-hydroxylated UiO-66(Zr) are very similar, exhibiting almost identical uptakes across the full pressure range studied. At low loading, xylene molecules were

found to be localized almost exclusively in the tetrahedral cavities of the MOF, in which oX-framework interactions are significantly enhanced compared to pX and mX (6-7 kJ/mol stronger; Figure 3), in agreement with the higher enthalpy of adsorption reported in literature for oX[19, 23]. In addition, the more compact oX isomer can explore these cavities more easily, with almost 1.5 times the number of accessible adsorption locations within the pore compared to mX and pX (see SI). Thus, the high uptake of oX at low pressure and the strong preference of the MOF for oX in competitive adsorption is a result of a strong energetic preference combined with a non-negligible entropic driving force.

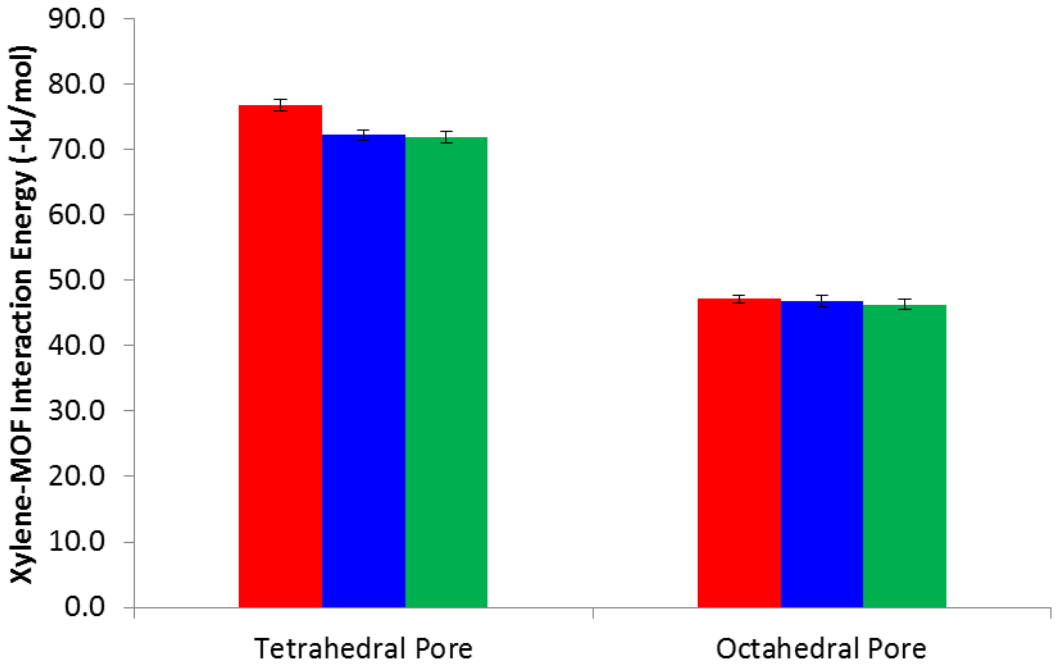

Figure 3 – Xylene-MOF interaction energies calculated per pore in the de-hydroxylated form from NVT MC simulations in the smaller, tetrahedral cavity (diameter 6.6 Å) and larger, octahedral cavity (diameter 7.5 Å) for oX (red), pX (blue) and mX (green).

The electrostatic contribution to the xylene-framework interaction in the tetrahedral pore types was found to be slightly repulsive and of a similar magnitude for all isomers (+0.25 to +1.5 kJ/mol), indicating that van der Waals interactions are responsible for the increase in oX-UiO-66(Zr) interaction energy. Examination of simulation snapshots shows that the origin of this enhancement lies in the ability of oX to position both methyl groups relatively centrally in the pore, allowing a strong interaction with the BDC linkers (Figure 4). In the case of both pX and mX, one or both of the methyl groups are forced away from the center of the pore towards the less energetically favorable pore window – that is, the methyl groups of pX and mX are interacting strongly with only a few framework atoms within the pore window and relatively weakly with the rest of the framework atoms which define the tetrahedral cavity, whereas those of oX are interacting relatively strongly with all six surrounding BDC ligands.

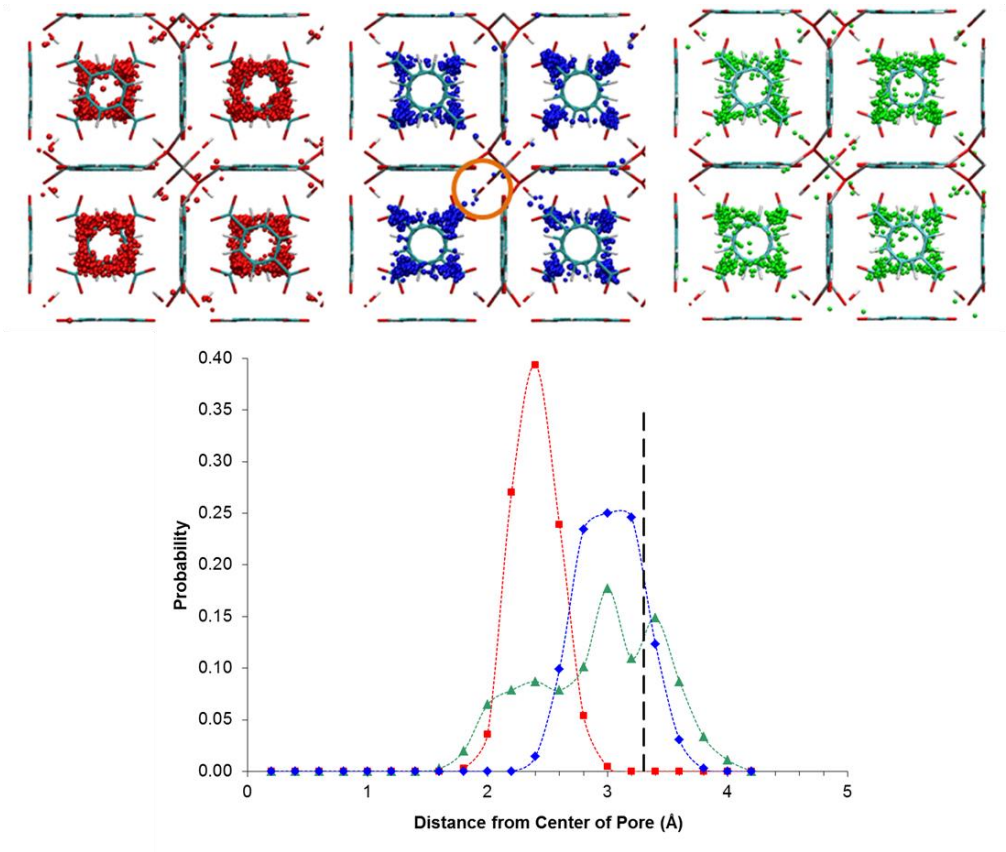

Figure 4 - Top: Observed locations of the methyl groups of oX (red), pX (blue) and mX (green) within UiO-66(Zr) in single component adsorption at 1 Pa. Each dot represents the position of a methyl group over the duration of the simulation. The pore windows are located towards the corners of each pore (e.g. the orange circle in the centre image). Bottom: Corresponding number probability distribution of the methyl groups as a function of radial distance from the centre of the tetrahedral cavity. Lines have been added to guide the eye. The radius of the tetrahedral pore is indicated by the black, dashed line.

None of the snapshots revealed any evidence of xylene molecules taking up a position parallel to one of the BDC linkers, indicating that π-π interactions do not play a significant role in the low-pressure adsorption properties for any of the isomers. Further investigation using a modified version of the Kh_d toolset [32] showed that while none of the isomers are sterically restricted from

accessing orientations which allow π-π interactions with the framework, these orientations are not energetically favorable, resulting in much lower xylene-MOF interaction energies (see Supporting Information).

While the strong preference for *ortho*-xylene observed in vapor-phase quaternary breakthrough experiments[6] and both liquid-phase binary and ternary breakthrough experiments[4] is correctly predicted in the present work, the situation is less clear in the case of pX-mX mixtures. In the vapor-phase work of Barcia *et al* [6], the MOF was unable to discriminate between mX and pX. In the later work of Moreira *et al* [4], however, UiO-66(Zr) was found to be weakly selective towards mX in both binary mX/pX and ternary oX/mX/pX breakthrough ($S_{pX\text{-}mX} = 0.9$). It should be noted that the studies of Moreira *et al* [4] were carried out in the liquid phase with heptane as a solvent which results in competitive adsorption of heptane and the xylene isomers. A direct comparison with the simulation is therefore difficult. In the quaternary (pX-mX-oX-ethylbenzene) competitive simulations reported by Granato *et al* [24], the MOF exhibited a slight preference for either pX or mX, depending on which force field was selected to describe the xylene isomers. In the present work, the MOF was found to be essentially non-selective (Figure 2).

The inability of the MOF to discriminate between pX and mX at equilibrium is a direct result of the almost identical xylene-MOF interaction energies for pX and mX in both types of cavity present in UiO-66(Zr) (Figure 3), suggesting that the mX-selectivity observed experimentally is unlikely to be enthalpic in nature. In order to fully understand the selectivity of UiO-66(Zr) for oX and the behavior of the pX-mX mixture observed in breakthrough experiments[4, 6, 19], it is necessary to assess the adsorption kinetics and diffusivity of the three isomers in the MOF. Additionally, it is clear that based on the crystallographic structure of UiO-66(Zr), the limiting pore window diameter in the static MOF (4-5 Å) is too small to permit the passage of xylene molecules (the

kinetic diameter of the slimmest isomer, pX, is 6.7 Å) and that some degree of structural flexibility is required to enable xylene molecules to diffuse through the MOF. In order to address these points, molecular dynamics (MD) simulations were undertaken in both rigid and flexible UiO-66(Zr), allowing both the underlying diffusion mechanism to be identified and the relative mobility of the three isomers to be assessed.

In MD simulations in which the MOF is kept rigid, none of the xylene isomers were observed moving from one pore to the next, either at 300 K or 500 K. Even in MD simulations in UiO-66(Zr) at 300 K using a force field which allows framework flexibility, xylene molecules remained localized within their starting cages and no transitions between cavities were observed. The movement of xylene isomers between cages was only observed in MD simulations undertaken at elevated temperatures (500 – 1000 K), from which we are able to qualitatively explain both the structural movements which facilitate xylene diffusion and the significant differences in transition rate and mechanism between the three isomers.

The window connecting adjoining pores is defined by three BDC linkers arranged in a triangular fashion (Figure 5; left) which, when held rigid, create a hexagonal window with an incircle diameter of ~4-5 Å. When the framework is treated as flexible, the window-defining BDC linkers are able to undergo a rotation around the (OOC)-(COO) axis and twisting and buckling of the aromatic-substituent improper torsion center (Figure 5). The combination of these two motions, induced by interaction between the linkers and adsorbed xylene molecules, causes the window to enlarge and change shape (Figure 5; right), allowing the xylene molecule to move from one pore to the next.

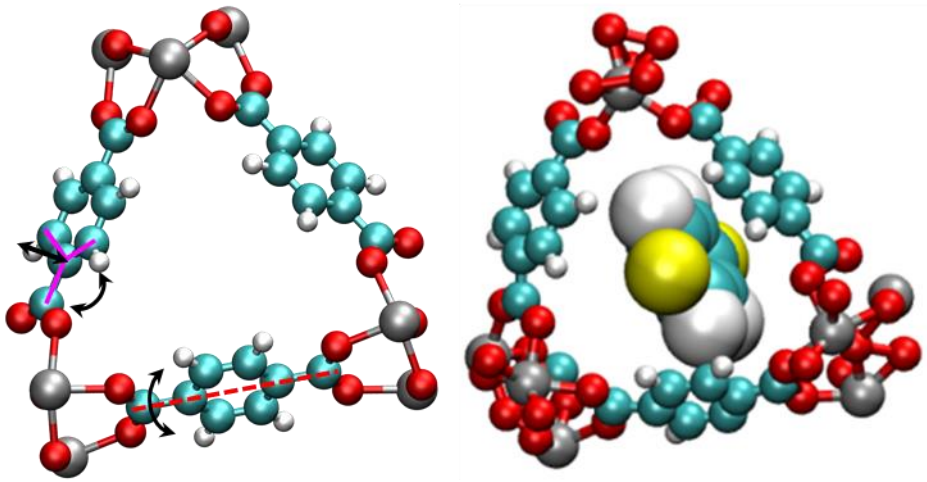

Figure 5 - BDC linkers forming the window present in UiO-66(Zr) in the equilibrium atomic positions used in the rigid structure (left) and during deformation of the window in the presence of pX in MD simulations using a flexible force field (right). The important rotation axis (red dashed line) and torsion center (pink solid lines) are highlighted. Color scheme: C – cyan; H – white; O – red; Zr – grey; CH_3 group – yellow.

In the case of pX and mX, xylene molecules were seen to move between cage types at temperatures of 500 K and above (Figure 6). This transition remained extremely rare at 500 K, with each pX molecule undergoing an average of 0.11 transitions per nanosecond. As the temperature was increased, the transition rate increased to 1.13 molecule^{-1} ns^{-1} and 1.52 molecule^{-1} ns^{-1} at 800 K and 900 K respectively. mX was found to be much less mobile than pX, with an observed transition rate of 0.02 molecule^{-1} ns^{-1} at 500 K – a factor of six lower than pX. oX was found to be the least mobile of the three isomers and transitions were only observed above 800 K.

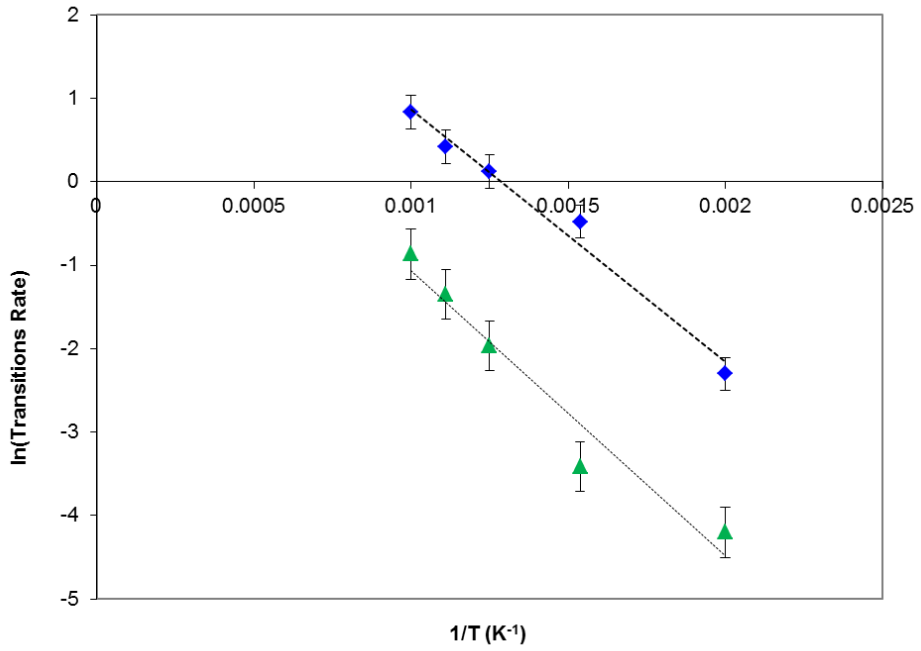

Figure 6 - Temperature-dependence of the cage-to-cage transition rate of pX (blue) and mX (green) in flexible UiO-66(Zr). Dotted lines are those of best fit for determination of Arrhenius coefficients.

The increase in the pX and mX transition rate constant with temperature is well described by the standard Arrhenius equation, from which the activation energy associated with the movement of molecules between cages at low loading was calculated to be 25.2 ± 0.5 kJ/mol for pX and 28.4 ± 1.4 kJ/mol for mX. In contrast to pX and mX, the movement of oX from cage to cage remained an extremely rare event even at elevated temperature. For oX, only two transition events were observed per 10 ns simulation run at 800 K, and only three at 900 K. While it is impossible to accurately determine activation energies from this data, the two order of magnitude difference in transition rate between pX and oX suggests that the activation energy for oX is approximately 20 kJ/mol higher.

Surprisingly, the overall order of mobility observed in MD simulations (pX > mX >> oX) does not correspond to the order of kinetic diameters of the isomers (pX < oX < mX). The reason for this apparent discrepancy lies in the fact that the kinetic diameter does not take into account the rotation of the molecule during the transition event. pX was seen to move through the window with minimal rotation of the isomer – the only observed rotation was around the long (CH_3-CH_3) axis of the molecule (Figure 7; top). The required window diameter (critical diameter) for this motion is approximately 6.7 Å. While moving through the pore window, mX follows a different path, experiencing rotation around the center of the aromatic ring, perpendicular to the long axis of the molecule (Figure 7; middle). As a result of the rotation of the molecule, the critical diameter is much less than the measured kinetic diameter (7.4 Å compared to 7.8 Å). The lower mobility of mX compared to pX is thus primarily a result of the larger critical diameter and the increased distortion of the framework required to allow passage through the window.

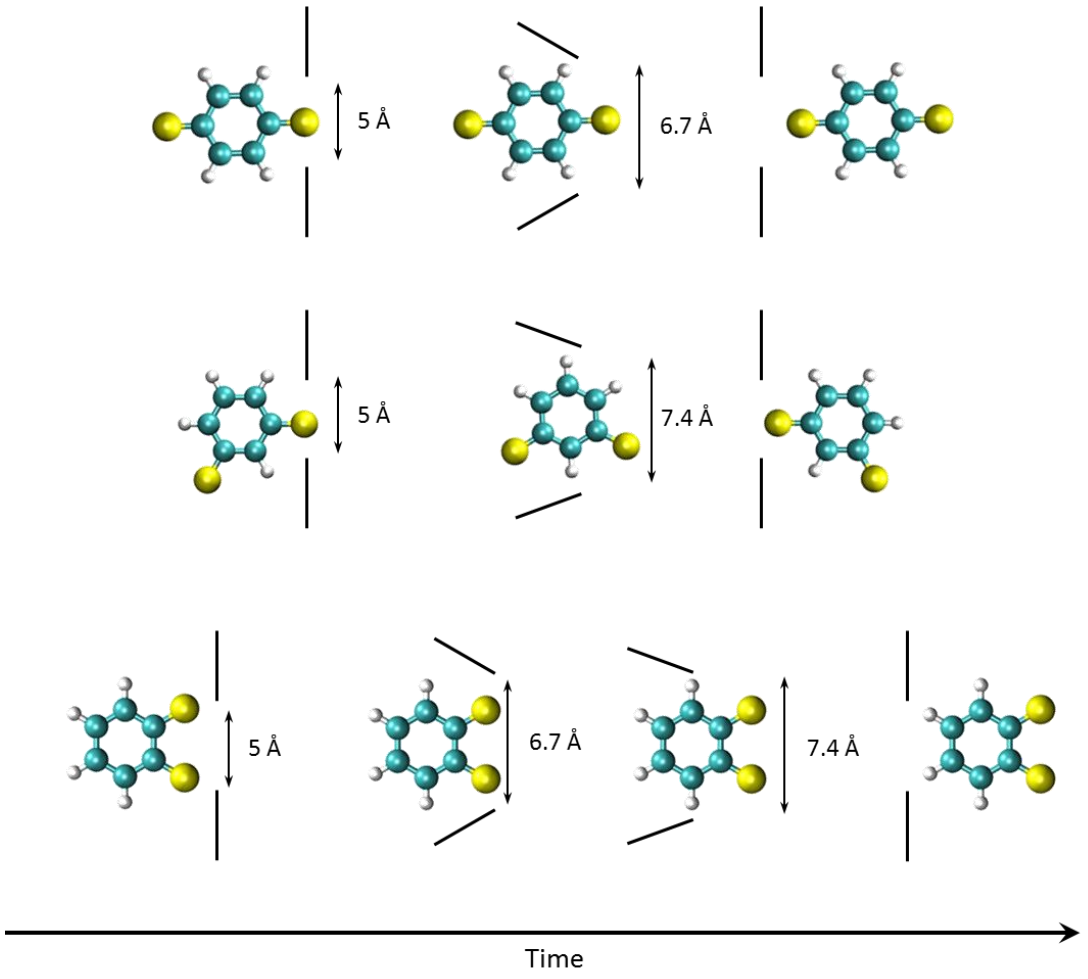

Figure 7 – Schematic representation of the movement of of pX (top), mX (middle) and oX (bottom) through the window of UiO-66(Zr). The relative orientation of the linkers is shown by the solid black lines while the minimum window diameter for each of the steps is indicated alongside. Vertical black lines correspond to the equilibrium linker orientation. Color scheme: C – cyan; H – white; CH_3 group – yellow.

The smallest critical diameter which oX is capable of presenting is also 7.4 Å and, given that the window is capable of admitting mX, the movement of oX should not be restricted from a geometric perspective. The primary difference between oX and the other isomers is that the two methyl groups are adjacent, existing as a pair rather than single protruding entities. The pore window has

an equilibrium diameter of roughly 4 - 5 Å, while the single methyl group has a diameter of 3.8 Å in these simulations. It is clear that even without framework distortion the single methyl group is able to enter the pore window. In contrast, the methyl pair on oX has a combined diameter of approximately 6.7 Å – too large to enter into the pore window without prior distortion of the framework (Figure 7; bottom).

The single methyl groups present on mX and pX thus act as a wedge whose presence within the pore window is able to induce further distortion of the framework, enlarging the window and enabling the rest of the molecule to pass through. The low mobility of oX is therefore a result of the molecule being forced to wait for the window to spontaneously enlarge before any portion of the molecule is able to enter the window. The ability of pX and mX to position their methyl groups within the pore windows even when the structure is at equilibrium is supported by the GCMC results presented earlier, wherein both pX and mX were observed to preferentially locate one or both methyl groups in the pore window (Figure 4). In GCMC simulations, this had the effect of reducing the adsorption affinity of the MOF for pX and mX compared to oX. The complete encapsulation of the oX molecule within the pore thus enhances the equilibrium selectivity, while simultaneously reducing the mobility of oX within the framework compared to pX and mX, introducing an additional kinetic selectivity to the system. The breakthrough experiments of Moreira *et al* [4] provide some evidence of a considerably lower transition rate of oX compared to the other two isomers, with oX demonstrating noticeably more disperse breakthrough profiles than those of pX and mX. While ethylbenzene (EB) was not considered in the present work, it may be expected that the ethyl group – being similarly sterically unhindered – would allow it to follow a similar transition mechanism to pX and mX, evidenced in the sharp peaks for pX, mX and EB observed in the vapor-phase work of Barcia *et al*[6]. Furthermore, one may expect that while the

longer alkyl group in EB may prevent the molecule from being as well encapsulated as oX, the additional configurational freedom experienced by EB compared to the other isomers may play a significant role and future work should seek to explore these aspects of the behavior of EB within UiO-66. Additionally it is important to note, however, that the UiO-66 system has been shown to be susceptible to missing linker defect formation[33-34] and further work is required to quantify the influence of these defects on xylene adsorption and diffusion.

CONCLUSIONS

In this work, we carried out a detailed computational study of the unusual behavior of xylene isomers in the metal-organic framework UiO-66(Zr), augmenting GCMC simulations of adsorption with NVT MC, complementary geometric tools and MD simulations in both rigid and flexible models of the framework. We demonstrate that such a combined computational approach is required to fully understand the previously reported selectivity of the MOF for oX –shown here to be strongly dependent on both the equilibrium and kinetic properties of the xylene-MOF system.

The clear preference of the MOF for oX observed in experiment was correctly predicted by simulation and, furthermore, the calculated xylene-framework interactions are in good agreement with the enthalpies of adsorption determined experimentally[19, 23]. It was shown that the enhanced xylene-framework interactions observed for oX in comparison to the other two isomers arises from neither π-π nor electrostatic interactions but is a result of the complete encapsulation of the oX molecule within the tetrahedral cavities. Geometric restrictions force the other isomers to take up less energetically favorable positions with one or both methyl groups located in the pore windows.

While xylene adsorption in UiO-66(Zr) was well-predicted when the framework is kept rigid (not exhibiting any large scale breathing behavior or gate opening effects, UiO-66 is considered to be a rigid MOF), the flexibility of the MOF and movement of atoms away from their

crystallographic positions was found to be crucial in allowing xylene molecules to diffuse through the structure. The movement of xylene molecules from one cage to the next was only observed during simulations using a flexible framework. The ability of the BDC linkers to both rotate and flex in response to interaction with adsorbed xylene molecules was seen to result in an enlargement of the window diameter, enabling xylenes to pass from one pore to the next. This transition was found to be hindered considerably in the case of oX, whose adjacent methyl groups are less able to induce the enlargement of the window than the individual methyl groups of pX and mX. The overall high oX-selectivity observed in breakthrough experiment is therefore a combination of both a kinetic contribution and the previously established enthalpic preference. The higher activation energy for the movement of mX through the pore network when compared to pX, combined with the lack of clear preference for either component in GCMC simulations, suggests that the slight selectivity towards mX observed in some experiments is also kinetic rather than enthalpic in nature.

While the present work highlights the key role which computational techniques have to play in identifying the structural features integral to adsorption-based xylene separations, the strong influence of framework flexibility on xylene behavior reported herein – and recently demonstrated for the similarly 'rigid' MIL-47 and MOF-48 systems[35] – provides further evidence that the incorporation of flexibility in molecular simulation must be addressed when screening MOFs computationally for industrial adsorption applications.

SUPPORTING INFORMATION

Pore size distributions for hydroxylated and dehydroxylated UiO-66(Zr); pX dimer formation in hydroxylated UiO-66(Zr); calculation of the accessible adsorption sites for the three isomers, additional simulation details of evaluation of π-π stacking of xylenes in UiO-66(Zr).

ACKNOWLEDGMENTS

The research leading to these results has received funding from the European Community's Seventh Framework Programme (FP7/2007-2013) under grant agreement No. 228862. This work has made use of the resources provided by the Edinburgh Compute and Data Facility (ECDF) (http://www.ecdf.ed.ac.uk/). The authors wish to thank Prof. Guillaume Maurin and Dr. Qingyuan Yang for providing the structure and partial atomic charges for hydroxylated UiO-66(Zr) and Dr. Naseem Ramsahye for guidance on the implementation of MD simulations in flexible UiO-66(Zr) in DL_POLY.

AUTHOR INFORMATION

The authors confirm that the manuscript through contributions from all authors and declare no competing financial interest.

*Corresponding author: T.Duren@bath.ac.uk

REFERENCES

1. Sholl, D. S.; Lively, R. P., Seven Chemical Separations to Change the World. *Nature* **2016**, *532*, 435-437.
2. Cannella, W. J., Xylenes and Ethylbenzene. In *Kirk-Othmer Encyclopedia of Chemical Technology*, John Wiley & Sons, Inc.: 2000.
3. Kurup, A. S.; Hidajat, K.; Ray, A. K., Optimal Operation of an Industrial-Scale Parex Process for the Recovery of P-Xylene from a Mixture of C-8 Aromatics. *Industrial & Engineering Chemistry Research* **2005**, *44*, 5703-5714.
4. Moreira, M. A., et al., Reverse Shape Selectivity in the Liquid-Phase Adsorption of Xylene Isomers in Zirconium Terephthalate Mof Uio-66. *Langmuir* **2012**, *28*, 5715-5723.
5. Alaerts, L.; Maes, M.; Giebeler, L.; Jacobs, P. A.; Martens, J. A.; Denayer, J. F. M.; Kirschhock, C. E. A.; De Vos, D. E., Selective Adsorption and Separation of Ortho-Substituted Alkylaromatics with the Microporous Aluminum Terephthalate Mil-53. *J. Am. Chem. Soc.* **2008**, *130*, 14170-14178.
6. Barcia, P. S.; Guimaraes, D.; Mendes, P. A. P.; Silva, J. A. C.; Guillerm, V.; Chevreau, H.; Serre, C.; Rodrigues, A. E., Reverse Shape Selectivity in the Adsorption of Hexane and Xylene Isomers in Mof Uio-66. *Microporous and Mesoporous Materials* **2011**, *139*, 67-73.

7. El Osta, R.; Carlin-Sinclair, A.; Guillou, N.; Walton, R. I.; Vermoortele, F.; Maes, M.; de Vos, D.; Millange, F., Liquid-Phase Adsorption and Separation of Xylene Isomers by the Flexible Porous Metal-Organic Framework Mil-53(Fe). *Chem. Mat.* **2012**, *24*, 2781-2791.
8. Gu, Z.-Y.; Jiang, D.-Q.; Wang, H.-F.; Cui, X.-Y.; Yan, X.-P., Adsorption and Separation of Xylene Isomers and Ethylbenzene on Two Zn−Terephthalate Metal−Organic Frameworks. *The Journal of Physical Chemistry C* **2009**, *114*, 311-316.
9. Trens, P.; Belarbi, H.; Shepherd, C.; Gonzalez, P.; Ramsahye, N. A.; Lee, U. H.; Seo, Y. K.; Chang, J. S., Adsorption and Separation of Xylene Isomers Vapors onto the Chromium Terephthalate-Based Porous Material Mil-101(Cr): An Experimental and Computational Study. *Microporous and Mesoporous Materials* **2014**, *183*, 17-22.
10. Vermoortele, F., et al., P-Xylene-Selective Metal-Organic Frameworks: A Case of Topology-Directed Selectivity. *J. Am. Chem. Soc.* **2011**, *133*, 18526-18529.
11. Gee, J. A.; Zhang, K.; Bhattacharyya, S.; Bentley, J.; Rungta, M.; Abichandani, J. S.; Sholl, D. S.; Nair, S., Computational Identification and Experimental Evaluation of Metal–Organic Frameworks for Xylene Enrichment. *The Journal of Physical Chemistry C* **2016**.
12. Cavka, J. H.; Jakobsen, S.; Olsbye, U.; Guillou, N.; Lamberti, C.; Bordiga, S.; Lillerud, K. P., A New Zirconium Inorganic Building Brick Forming Metal Organic Frameworks with Exceptional Stability. *J. Am. Chem. Soc.* **2008**, *130*, 13850-13851.
13. Valenzano, L.; Civalleri, B.; Chavan, S.; Bordiga, S.; Nilsen, M. H.; Jakobsen, S.; Lillerud, K. P.; Lamberti, C., Disclosing the Complex Structure of Uio-66 Metal Organic Framework: A Synergic Combination of Experiment and Theory. *Chem. Mat.* **2011**, *23*, 1700-1718.
14. Serre, C.; Millange, F.; Thouvenot, C.; Nogues, M.; Marsolier, G.; Louer, D.; Ferey, G., Very Large Breathing Effect in the First Nanoporous Chromium(Iii)-Based Solids: Mil-53 or Cr-Iii(Oh)Center Dot{O2c-C6h4-Co2}Center Dot{Ho2c-C6h4-Co2h}(X)Center Dot H2oy. *J. Am. Chem. Soc.* **2002**, *124*, 13519-13526.
15. Serre, C.; Millange, F.; Surblé, S.; Férey, G., A Route to the Synthesis of Trivalent Transition-Metal Porous Carboxylates with Trimeric Secondary Building Units. *Angewandte Chemie International Edition* **2004**, *43*, 6285-6289.
16. Kolokolov, D. I.; Stepanov, A. G.; Guillerm, V.; Serre, C.; Frick, B.; Jobic, H., Probing the Dynamics of the Porous Zr Terephthalate Uio-66 Framework Using H-2 Nmr and Neutron Scattering. *J. Phys. Chem. C* **2012**, *116*, 12131-12136.
17. Devautour-Vinot, S.; Maurin, G.; Serre, C.; Horcajada, P.; da Cunha, D. P.; Guillerm, V.; Costa, E. D.; Taulelle, F.; Martineau, C., Structure and Dynamics of the Functionalized Mof Type Uio-66(Zr): Nmr and Dielectric Relaxation Spectroscopies Coupled with Dft Calculations. *Chem. Mat.* **2012**, *24*, 2168-2177.
18. Yang, Q. Y.; Wiersum, A. D.; Jobic, H.; Guillerm, V.; Serre, C.; Llewellyn, P. L.; Maurin, G., Understanding the Thermodynamic and Kinetic Behavior of the Co2/Ch4 Gas Mixture within the Porous Zirconium Terephthalate Uio-66(Zr): A Joint Experimental and Modeling Approach. *J. Phys. Chem. C* **2011**, *115*, 13768-13774.
19. Chang, N.; Yan, X.-P., Exploring Reverse Shape Selectivity and Molecular Sieving Effect of Metal-Organic Framework Uio-66 Coated Capillary Column for Gas Chromatographic Separation. *Journal of Chromatography A* **2012**, *1257*, 116-124.
20. Santilli, D. S.; Harris, T. V.; Zones, S. I., Inverse Shape Selectivity in Molecular Sieves: Observations, Modelling, and Predictions. *Microporous Materials* **1993**, *1*, 329-341.
21. Denayer, J. F. M.; Ocakoglu, R. A.; Arik, I. C.; Kirschhock, C. E. A.; Martens, J. A.; Baron, G. V., Rotational Entropy Driven Separation of Alkane/Isoalkane Mixtures in Zeolite Cages. *Angewandte Chemie International Edition* **2005**, *44*, 400-403.
22. Bozbiyik, B.; Duerinck, T.; Lannoeye, J.; De Vos, D. E.; Baron, G. V.; Denayer, J. F. M., Adsorption and Separation of N-Hexane and Cyclohexane on the Uio-66 Metal-Organic Framework. *Microporous and Mesoporous Materials* **2014**, *183*, 143-149.

23. Duerinck, T.; Bueno-Perez, R.; Vermoortele, F.; De Vos, D. E.; Calero, S.; Baron, G. V.; Denayer, J. F. M., Understanding Hydrocarbon Adsorption in the Uio-66 Metal-Organic Framework: Separation of (Un)Saturated Linear, Branched, Cyclic Adsorbates, Including Stereoisomers. *J. Phys. Chem. C* **2013**, *117*, 12567-12578.
24. Granato, M. A.; Martins, V. D.; Ferreira, A. F. P.; Rodrigues, A. E., Adsorption of Xylene Isomers in Mof Uio-66 by Molecular Simulation. *Microporous and Mesoporous Materials* **2014**, *190*, 165-170.
25. Yang, Q.; Jobic, H.; Salles, F.; Kolokolov, D.; Guillerm, V.; Serre, C.; Maurin, G., Probing the Dynamics of Co2 and Ch4 within the Porous Zirconium Terephthalate Uio-66(Zr): A Synergic Combination of Neutron Scattering Measurements and Molecular Simulations. *Chem.-Eur. J.* **2011**, *17*, 8882-8889.
26. Mayo, S. L.; Olafson, B. D.; Goddard, W. A., Dreiding - a Generic Force-Field for Molecular Simulations. *J Phys Chem-Us* **1990**, *94*, 8897-8909.
27. Rappe, A. K.; Casewit, C. J.; Colwell, K. S.; Goddard, W. A.; Skiff, W. M., Uff, a Full Periodic-Table Force-Field for Molecular Mechanics and Molecular-Dynamics Simulations. *J. Am. Chem. Soc.* **1992**, *114*, 10024-10035.
28. Yang, Q. Y.; Wiersum, A. D.; Llewellyn, P. L.; Guillerm, V.; Serred, C.; Maurin, G., Functionalizing Porous Zirconium Terephthalate Uio-66(Zr) for Natural Gas Upgrading: A Computational Exploration. *Chem. Commun.* **2011**, *47*, 9603-9605.
29. Jorgensen, W. L.; Laird, E. R.; Nguyen, T. B.; Tiradorives, J., Monte-Carlo Simulations of Pure Liquid Substituted Benzenes with Opls Potential Functions. *Journal of Computational Chemistry* **1993**, *14*, 206-215.
30. Gupta, A.; Chempath, S.; Sanborn, M. J.; Clark, L. A.; Snurr, R. Q., Object-Oriented Programming Paradigms for Molecular Modeling. *Mol. Simul.* **2003**, *29*, 29-46.
31. Todorov, I. T.; Smith, W.; Trachenko, K.; Dove, M. T., Dl_Poly_3: New Dimensions in Molecular Dynamics Simulations Via Massive Parallelism. *J. Mater. Chem.* **2006**, *16*, 1911-1918.
32. Sarkisov, L., Toward Rational Design of Metal-Organic Frameworks for Sensing Applications: Efficient Calculation of Adsorption Characteristics in Zero Loading Regime. *J. Phys. Chem. C* **2012**, *116*, 3025-3033.
33. Wu, H.; Chua, Y. S.; Krungleviciute, V.; Tyagi, M.; Chen, P.; Yildirim, T.; Zhou, W., Unusual and Highly Tunable Missing-Linker Defects in Zirconium Metal–Organic Framework Uio-66 and Their Important Effects on Gas Adsorption. *J. Am. Chem. Soc.* **2013**, *135*, 10525-10532.
34. Cliffe, M. J.; Wan, W.; Zou, X.; Chater, P. A.; Kleppe, A. K.; Tucker, M. G.; Wilhelm, H.; Funnell, N. P.; Coudert, F.-X.; Goodwin, A. L., Correlated Defect Nanoregions in a Metal–Organic Framework. *Nat Commun* **2014**, *5*.
35. Gee, J. A.; Sholl, D. S., Effect of Framework Flexibility on C-8 Aromatic Adsorption at High Loadings in Metal-Organic Frameworks. *J. Phys. Chem. C* **2016**, *120*, 370-376.

TOC Graphic